

## Six-stroke spark-ignition engine fuelled with high-hydrogen content fuel: a theoretical thermodynamic analysis

### ARTICLE INFO

*This work presents a thermodynamic analysis of a six-stroke cycle implemented in Spark-Ignition (SI) engines. The cycle configuration comprises two distinct combustion phases: (1) initial combustion of a methane-hydrogen mixture under fuel-lean conditions ( $\lambda > 1$ ), yielding exhaust gases containing residual oxygen, followed by (2) secondary hydrogen injection during the expansion phase to facilitate complete utilization of the remaining oxidizer. The investigation evaluates the system's thermodynamic performance through parametric variation of both the fuel composition (methane/hydrogen,  $\text{CH}_4/\text{H}_2$  ratio) and the equivalence ratio during primary combustion. The results obtained indicate that the changes in the peak temperature of the second part of the cycle are small, up to 60 K relative to the mean value. The fuel mixture with  $\lambda = 3.0$  showed the highest cycle efficiency at 50.73%, indicating the best performance among all cases. According to the data, better performance can be achieved by optimizing cycle parameters such as regeneration, intercooling, pressure ratios, and component efficiencies in addition to raising the maximum temperature. In conclusion, better outcomes are not always guaranteed by higher temperatures. Increasing thermal input alone is not as important as designing and optimizing cycles efficiently.*

Received: 2 July 2025

Revised: 7 October 2025

Accepted: 21 October 2025

Available online: 22 November 2025

Key words: *hydrogen, renewable energy, thermodynamic parameters, SI engine, 6-stroke cycle*

This is an open access article under the CC BY license (<http://creativecommons.org/licenses/by/4.0/>)

### 1. Introduction

As the global demand for cleaner energy builds momentum, internal combustion engines (ICEs) remain a leading point of energy conversion in transportation and distributed power generation. However, their continued use falls under increasing concern due to greenhouse gas (GHG) emissions in the form of carbon dioxide ( $\text{CO}_2$ ) and nitrogen oxides ( $\text{NO}_x$ ), which are accountable for climate change and air pollution.

As a countermeasure, the combination of renewable energies with hydrogen-powered engines could be a promising path to a sustainable energy future, replacing the use of conventional non-renewable energy. While the combustion of hydrogen is carbon-free and increases thermal efficiency [12], it occurs at very high temperatures, which can result in high thermal  $\text{NO}_x$  formation.

However, under certain conditions, a reduction in power output can occur, and one reason for this is the need to burn hydrogen at a high excess air ratio due to the propensity of this fuel to experience excessively high cylinder pressure and knocking combustion. The higher the excess air ratio, the lower the calorific value of the fuel-air mixture feeding the combustion engine [5]. In addition, the higher combustion temperature of hydrogen can result in higher heat losses from the internal combustion engine, further reducing its efficiency, and also increasing  $\text{NO}_x$  emissions [4].

At the same time, it is worth noting that enriching natural gas or biogas with hydrogen brings tangible benefits to the performance of internal combustion engines. Previous studies have shown that hydrogen enrichment contributes to alleviating combustion instability issues in engines fuelled with gaseous blends, leading to a significant reduction in emissions [8]. Hydrogen, according to the literature, has the

ability to improve the coefficient of variation (COV) of indicated mean effective pressure (IMEP) and other properties when mixed with other fuels, such as natural gas, the latter being highly encouraged by several countries for use in internal combustion engines with a view to reducing global warming and pollutant emissions [2].

Within this framework, one alternative to sensibly improve the performance of engines burning  $\text{H}_2$ -rich fuels or pure  $\text{H}_2$  is to modify the thermodynamic cycle of the engine. Therefore, this paper presents a concept for implementing a six-stroke thermodynamic cycle for hydrogen combustion in an SI engine. The cycle parameters were calculated when using a hydrogen-methane mixture as fuel.

### 2. Properties of selected gaseous fuels

#### 2.1. Main properties of $\text{H}_2$ , biomethane and biogas

Governments around the world are paying closer attention to hydrogen, methane, and biogas as cleaner fuels for internal combustion engines, particularly in the context of the movement towards sustainable energy. One notable feature of hydrogen is that it burns cleanly, releasing no  $\text{CO}_2$  when it is used. Produced from various energy sources, it is considered a form of energy carrier. With unique properties, it is seen as promising for use in engines, such as its low density, wide flammability limits, and low minimum ignition energy. Also, certain mixtures can improve combustion stability. Special attention should be paid to its laminar burn rate, which under certain conditions can be up to six times higher than that of gasoline or methane [6, 13].

Biomethane, an upgraded form of biogas that increases its energy content, is a fuel that can be directly used in natural gas vehicles. Moreover, it can be injected into existing natural gas infrastructure and be used in transportation

in different regions [7], making it a convenient and cleaner-burning alternative to non-renewable fuels in SI engines. On the other hand, biogas is made through the anaerobic digestion of organic matter, a process that happens without oxygen. Before being used in engines, it must be upgraded to remove carbon dioxide and other impurities, the above-mentioned biomethane. It is an added benefit of being renewable, turning organic waste into a valuable source of clean energy. It stands out as a promising fuel in diesel engines, in addition to its potential for reducing emissions, although with lower performance values [1, 11].

Some of the main properties of  $H_2$  and  $CH_4$  include the Lower Heating Value (LHV) which range from  $\sim 120$  MJ/kg;  $\sim 10.8$  MJ/Nm<sup>3</sup>;  $\sim 50$  MJ/kg;  $\sim 35.8$  MJ/Nm<sup>3</sup> and the density at NTP (0°C, 1 atm), equals to 0.0899 kg/m<sup>3</sup> and 0.656 kg/m<sup>3</sup>, respectively [14]. Furthermore, another desirable property is the very fast flame propagation from  $H_2$ , which reduces combustion duration, leading to high isochoric efficiency [10]. As for biogas, with its wide range of energy applications, trace compounds can impact its use, with special attention to concentrations of volatile organic compounds (VOCs), for example [9].

Finally, in spark ignition (SI) Engines and other types of engines, it is important, among other things, to control the rapid increase in pressure within the engine, which can lead to knock. Knock is undesirable and a major challenge in the field [13], especially with fuel blends containing  $H_2$ .

## 2.2. Characteristics of the fuel-air mixture

The stoichiometric air–fuel ratio for hydrogen is 34.3 (kg/kg) compared to 14.3 for diesel and 17.2 for methane fuels. The engine's power output for a given fuel depends on the calorific value of the fuel-air mixture and the engine's thermodynamic efficiency. According to Fig. 1, the relative difference ( $\Delta e_{d,v}$  in %) of the calorific value of the hydrogen-air mixture in relation to selected fuels like biogas (with 60% of  $CH_4$  by vol.), methane, petrol and diesel oil in a range of air excess ratios. The relative difference in calorific value of the hydrogen-air mixture ( $e_{d,vH_2}$ ) compared to other fuel-air mixtures ( $e_{d,vf}$ ) is defined in Equation 1.

$$\Delta e_{d,v} = \left( 1 - \frac{e_{d,vf}}{e_{d,vH_2}} \right) 100\% \quad (1)$$

where:  $e_{d,vf}$ , J/Nm<sup>3</sup> – calorific value of selected fuel-air mixture,  $e_{d,vH_2}$ , J/Nm<sup>3</sup> – calorific value of the hydrogen-air mixture.

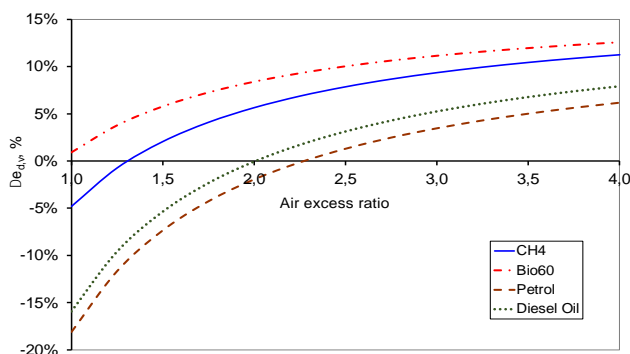


Fig. 1. Relative difference in calorific value of the fuel-air mixture of four selected fuels compared to hydrogen

The  $\Delta e_{d,v}$  results are expressed in % of the calorific value of the hydrogen-air mixture under normal conditions. From the data presented in Fig. 1, it is evident that hydrogen has the same energy potential in the combustible mixture ( $\Delta e_{d,v} = 0\%$ ) for different values of the excess air ratio. These are 1.3 for methane, 2 for diesel and 2.2 for gasoline, respectively. For a mixture of biogas and air, the calorific value is lower than that of pure hydrogen, even for a stoichiometric mixture.

## 3. Implementation of the six-stroke cycle in the SI engine

### 3.1. Introduction

The first conception of a six-stroke internal combustion engine was reported by Samuel Griffin in 1883, and many authors have since described and worked on six-stroke engines.

The basic idea from the literature is that waste heat is recovered, allowing a proportion of it to perform extra work. In a traditional six-stroke approach, the exhaust gases from the fourth stroke are not entirely exhausted into the environment (or are only partially exhausted) before compression occurs, followed by water injection to evaporate, which removes heat from the exhaust gas and the walls of the combustion chamber. Therefore, additional work is performed in the fifth stroke, and the charge is discharged to the environment in the sixth stroke [3].

### 3.2. Hydrogen-rich fuel utilization in a six-stroke cycle

One of the ways to sensibly improve the efficiency of engines burning  $H_2$ -rich fuels or pure  $H_2$  is to modify the thermodynamic cycle of the engine. The research proposed in this paper focuses on replacing the classic four-stroke cycle (4SCE) with a new six-stroke cycle (6SCE), as illustrated in Fig. 2.

The implementation of the six-stroke cycle in the SI engine is proposed as follows:

a) 1<sup>st</sup> stage of the cycle – in the first part of the cycle, the engine is fuelled with a lean air-fuel mixture. Various gaseous fuels, including those with hydrogen in their composition or pure hydrogen, are preferred. If pure hydrogen is used, a very lean mixture is required (an excess air ratio of at least three is assumed in this case). The fuel supply to the engine can be provided by a gas/air mixer or by using a gas injector in the engine intake manifold. The first part of the so-called ECO-CYCLE is realized analogously to the classic 4-stroke SI engine. After the engine is filled with a mixture of fuel and air, it is compressed and then ignited before the piston reaches top dead center (TDC). Subsequently, after the piston has passed through TDC, work is carried out in the engine cylinder, and torque is generated at the crankshaft.

b) 2<sup>nd</sup> stage of the cycle – after the work of the first part of the cycle has been carried out, the intake and exhaust valves remain closed and the exhaust gases containing oxygen are not released into the environment. At the end of the combustion process (e.g., in the expansion stage) or at the beginning of the next compression stage of the resulting exhaust gas, water injection is proposed to decrease the cylinder temperature. A partial reduction in temperature

should be achieved by injecting another dose of fuel. During this part of the cycle, direct injection of hydrogen into the engine cylinder is proposed, in such a quantity as to ensure a stoichiometric mixture with the oxygen remaining from the previous cycle in the exhaust. The resulting mixture undergoes compression, and another ignition is initiated before the piston reaches the TDC. Subsequently, another expansion occurs, and work is done in the engine cylinder, resulting in torque generation at the crankshaft.

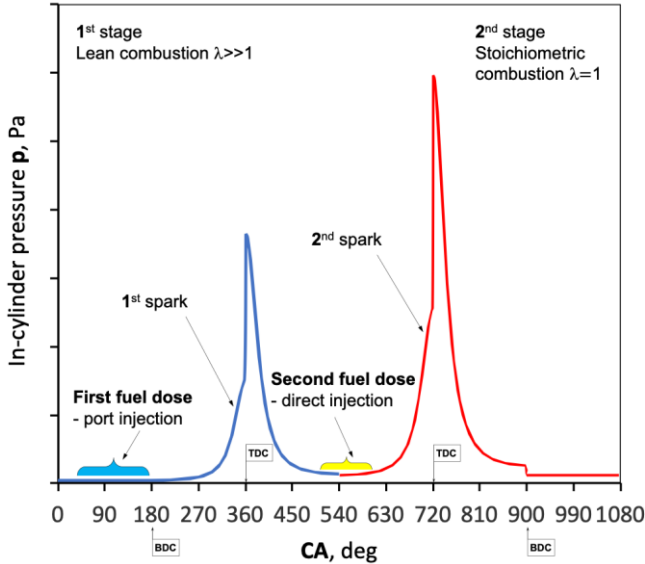


Fig. 2. The concept of six-stroke cycle implementation in a hydrogen rich fuel SI engine

To calculate the thermodynamic parameters of the 6-stroke cycle, it was necessary to determine the values of the input data. To determine the combustion stability of natural gas-hydrogen mixtures, experimental tests were carried out on a four-stroke spark-ignition engine with a compression ratio of 12.5. The content of hydrogen co-fired with methane was changed during the tests. The fuel mixture for which the engine operated stably, even with an excess air ratio above 2.5, was a mixture with 60% hydrogen by volume. For this work, simulation studies of the 6-stroke cycle were conducted for a fuel mixture of 60% H<sub>2</sub> and 40% CH<sub>4</sub>. Additionally, it was assumed that the range of variation for the excess air ratio would be between 1.3 and 3.

### 3.3. Calculation of thermodynamic parameters of a six-stroke cycle

The following assumptions and simplifications were made to determine the thermodynamic parameters of the six-stroke cycle:

- the compression and expansion of the load (i.e. the fuel/oxidant mixture and the exhaust gas) are isentropic
- the combustion process is simulated by isochoric heat input (in the first as well as in the second stage of the cycle), without heat losses to the environment.

The shape of the 6-stroke cycle on the pV diagram, along with its characteristic points, is shown in Fig. 3.

In the first stage of the cycle the fuel is a mixture of hydrogen and methane. Considering the mole fraction of each component, they will be defined in the following equations

as H<sub>2</sub> and CH<sub>4</sub>, respectively. Based on stoichiometry and considering the variable value of the excess air coefficient ( $\lambda$ ), the actual amount of air needed to burn the fuel is presented in Equation 2:

$$n'_{a1} = \lambda \frac{(2\text{CH}_4 + \frac{1}{2}\text{H}_2)}{Z_{\text{O}_2,a}}, \frac{\text{kmol}_f}{\text{kmol}_a} \quad (2)$$

where: H<sub>2</sub>, CH<sub>4</sub>, – molar content of H<sub>2</sub> and CH<sub>4</sub> in the fuel, Z<sub>O<sub>2</sub>,a</sub>, – molar content of O<sub>2</sub> in the air.

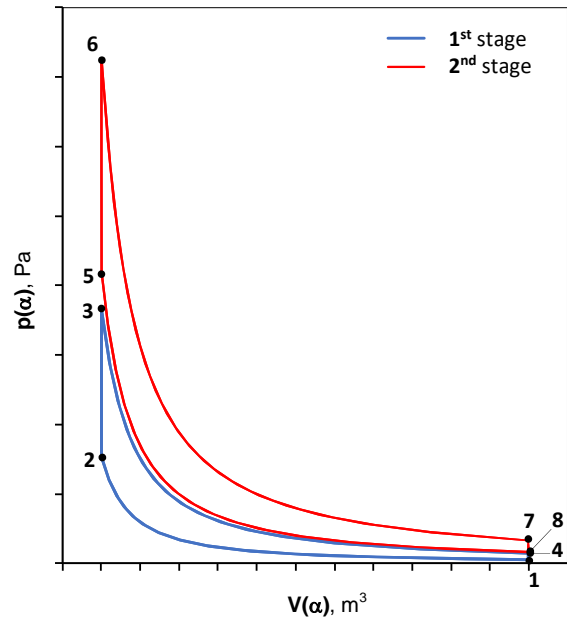


Fig. 3. The characteristic points of six-stroke cycle in p, V diagram

Using the initial cycle thermodynamic parameters, the molar quantity of working medium in the point “1” can be calculated from the Equation of state as below:

$$n_{1\text{mix}} = \frac{p_1 V_1}{(MR)T_1}, \frac{\text{kmol}_{\text{mix}}}{\text{cycle}} \quad (3)$$

where: p<sub>1</sub>, V<sub>1</sub>, T<sub>1</sub> – in cylinder parameters when the piston is in the BDC (suction stroke of 1<sup>st</sup> cycle stage).

Considering Equations (2) and (3), and the substance balance equation, the air and fuel mass for one engine cycle can be expressed by the following Equations:

$$m_{a1} = m_{f1} n'_{a1} \frac{M_a}{M_f} \left( 1 + \frac{M_{\text{H}_2\text{O}}}{M_a} X_{za} \right), \frac{\text{kg}_a}{\text{cycle}} \quad (4)$$

$$m_{f1} = \frac{p_1 V_1}{\left[ 1 + \frac{\lambda (2\text{CH}_4 + \frac{1}{2}\text{H}_2) (1 + X_{za})}{Z_{\text{O}_2,a}} \right] (MR)T_1}, \frac{\text{kg}_f}{\text{cycle}} \quad (5)$$

where: M<sub>a</sub>, M<sub>f</sub>, M<sub>H<sub>2</sub>O</sub>, kg/kmol – molar weight of air, fuel and H<sub>2</sub>O, X<sub>za</sub>, kmol<sub>H<sub>2</sub>O</sub>/kmol<sub>a</sub> – air moisture content.

The pressure during the compression and expansion stroke is calculated based on the isentropic transformation and expressed as a function of engine crank angle. These calculations finally yield the results of pressure at the 2<sup>nd</sup> and 4<sup>th</sup> points of the cycle. Cylinder volume changes for variable crankshaft angle were calculated based on the

geometry of the engine piston-crank system. In Table 1, the engine geometry adopted in the calculations is shown.

Table 1. Engine geometry

Bore, D, mm	86.0
Stroke, S, mm	69.0
Connecting rod, L, mm	117.0
Swept volume, $V_s, m^3$	0.000401
Number of cylinders	1.0
Compression ratio, $\epsilon$	12.5

Once the pressure  $p_2$  is calculated, the temperature  $T_2$  is determined using the thermal equation of state. The energy balance is then used to calculate the temperature value  $T_3$  using the following Equation:

$$T_3 = \frac{m_{f1} LHV_{f1}}{m_{1mix} c_v(T_{2-3})} + T_2 \quad (6)$$

where:  $LHV_{f1}$ , kJ/kg – lower heating value of the fuel,  $c_v(T_{2-3})$ , kJ/kgK – specific heat of the working medium during the heat supply process under constant volume,  $m_{1mix}$ , kg/cycle – mass of the working medium, the sum of fuel  $m_{f1}$  and air  $m_{a1}$ .

Then, the pressure in the circuit after the heat input is calculated by Equation 7:

$$p_3 = \frac{m_{1mix}(MR)T_3}{M_3 V_2} \quad (7)$$

where:  $V_2 = V_3, m^3$  – the min cycle volume (clearance volume),  $M_3$ , kg/kmol – molar mass of the working medium for its current molar composition.

The pressure  $p_4$  and temperature  $T_4$  are then calculated. In the current analysis, water injection was not implemented; hence, the temperature  $T_4$  is derived from the pressure at the end of the expansion and the amount of heat taken away by the hydrogen introduced at this point as fuel for the second part of the cycle.

The parameters for the second stage of the cycle are calculated analogously, but the oxidant is the residual oxygen from the exhaust of the first stage.

#### 4. Results

Using the calculation methodology given in section 3, a six-stroke cycle was simulated, assuming variable combustion conditions in the first part of the cycle. The variable parameter was the excess air ratio in the 1-st cycle stage. The values were changed from 1.3 to 3 with a value step of 0.2. In Figure 4, the post-combustion temperature values are shown in the first and second stages of the 6-stroke cycle. The results are shown as a function of the excess air factor used in the first stage of the cycle. Combustion in the second cycle stage was stoichiometric. The results obtained indicate that the changes in the peak temperature of the second part of the cycle are small, up to 60 K relative to the mean value.

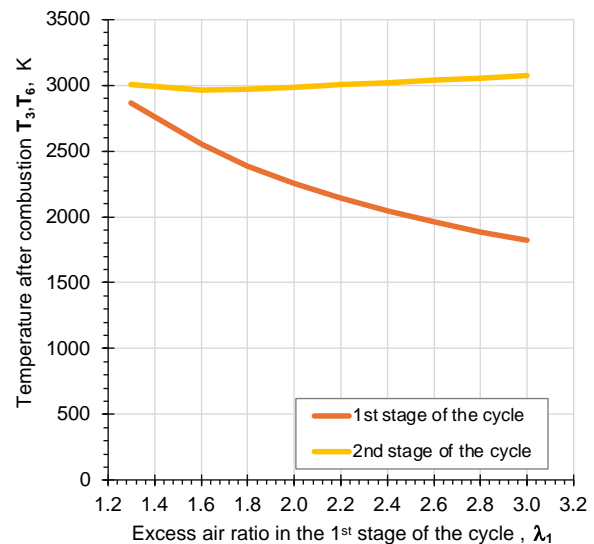
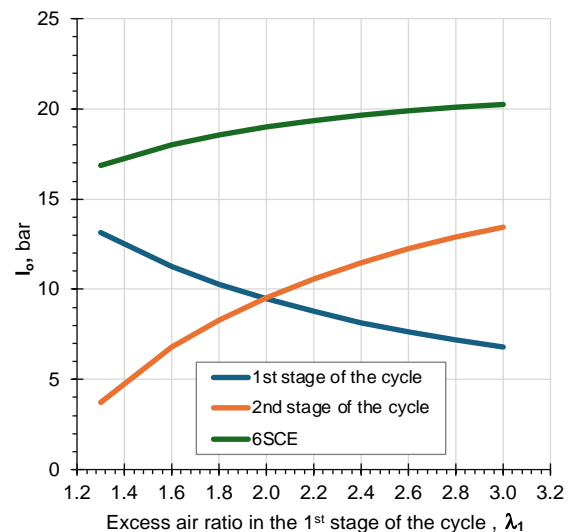
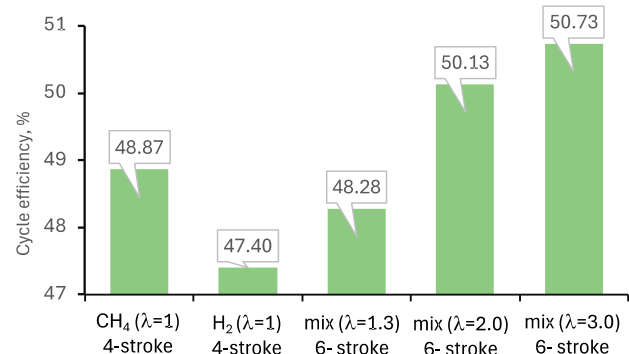

 Fig. 4. Temperature after combustion of 1<sup>st</sup> and the 2<sup>nd</sup> stage the 6-stroke cycle as function of the excess air ratio in the 1<sup>st</sup> cycle stage

 Fig. 5. Specific work of 1<sup>st</sup>, 2<sup>nd</sup> stage the 6-stroke cycle and whole cycle (6SCE) as function of the excess air ratio in the 1<sup>st</sup> cycle stage


Fig. 6. Comparison between 4-stroke and 6-stroke cycle efficiency

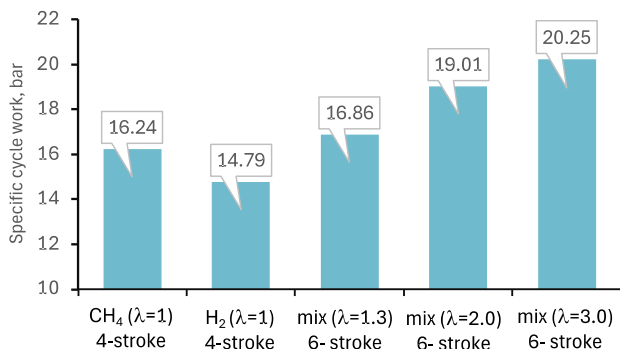


Fig. 7. Comparison between 4-stroke and 6-stroke specific cycle work

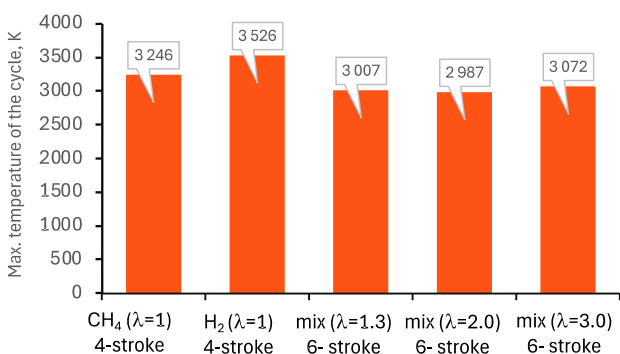


Fig. 8. Comparison between 4-stroke and 6-stroke maximum cycle temperature

In Figure 5, the specific work of the 1<sup>st</sup>, 2<sup>nd</sup> stage of the 6-stroke cycle and the whole cycle (6SCE) is shown as a function of the excess air ratio in the 1<sup>st</sup> cycle stage. The specific work was calculated as the ratio of the work performed by the working medium in the 1<sup>st</sup> and 2<sup>nd</sup> cycle stages to the engine's swept volume. As the excess air ratio increased, the specific work of the 1<sup>st</sup> stage decreased, while the specific work of the 2<sup>nd</sup> stage increased. The total specific work of the 6SCE increased slightly and then remained constant, indicating improved overall efficiency due to increased excess air.

Figures 6 to 8 express the comparison of the chosen parameters among the 4-stroke pure CH<sub>4</sub>, 4-stroke pure H<sub>2</sub> combustion and the 6-stroke cycle with 60 H<sub>2</sub> and 40 CH<sub>4</sub> % by vol. in the first stage and pure H<sub>2</sub> stoichiometrically combusted in the second stage. From Fig. 6, the mix with  $\lambda = 3.0$  showed the highest cycle efficiency at 50.73%, indicating the best performance among all cases. The pure H<sub>2</sub> result could be used as a baseline or a less effective configuration that might not have all the improvements. Depending on the application, the 3.33 percentage point difference in efficiency between the lowest (case H<sub>2</sub>) and the highest (mix with  $\lambda = 3.0$ ) can be substantial. The mix with  $\lambda = 3.0$  also produced the highest specific cycle work

at 20.25 bar in Fig. 7, demonstrating the most efficient work output per cycle swept volume. The specific cycle work expresses the equivalent of the indicated mean effective pressure of a real engine. A higher value for this parameter also means a higher output power of the engine.

The combustion of the fuels analyzed in the 6-stroke cycle allows a higher power output to be achieved relative to the 4-stroke cycle without the need for supercharging or turbocharging. In addition to the previous figures on cycle efficiency and specific cycle work, Fig. 8 shows the maximum cycle temperatures for the five distinct cases (1–5). Despite having the highest temperature in the 4-stroke cycle, pure H<sub>2</sub> also had the lowest specific cycle work (14.79 bar) and efficiency (47.4%). On the other hand, mix with  $\lambda = 3.0$  combusted in 6-stroke cycle at a moderate maximum temperature (3072 K) and had the highest efficiency (50.73%) and specific work (20.25 bar). According to the results of simulation calculations, better performance can be achieved by using a 6-stroke thermodynamic cycle. However, better outcomes are not always guaranteed by higher temperatures, due to thermodynamic and operational implications, thermal stress, etc. Increasing thermal input alone is not as important as designing and optimizing cycles efficiently.

Finally, to improve thermal efficiency in engines, in addition to the thermodynamic control and optimization of the process performed in this study, other approaches and solutions need to be developed.

Therefore, according to researchers, one such approach could be the use of multilayer coatings in the engine chamber. This technology could achieve greater thermal efficiency in internal combustion engines, and the literature points to the potential of this solution and the need for further research and analysis [15].

## 5. Conclusion

The mix with  $\lambda = 3.0$  (in the first stage of the six-stroke cycle) exhibited the best overall performance, reaching the highest specific work (20.25 bar) and cycle efficiency (50.73%) at a moderate maximum temperature (3072 K). On the other hand, H<sub>2</sub> performed the worst, despite having the highest temperature (3526 K). This is less than 500,000 lower than the stoichiometric combustion of pure hydrogen in a 4-stroke cycle. As the combustion in the second part of the 6-stroke cycle is stoichiometric, the use of such a solution in an actual internal combustion engine enables the use of a three-way catalyst converter in the exhaust system. This will allow the operation of the hydrogen-burning engine with high IMEP and efficiency, as well as reduced emissions of NO<sub>x</sub>, CO, and HC.

## Acknowledgements

We would like to thank the National Council for Scientific and Technological Development – CNPq, process number 441811/2023-0, the Federal University of Pelotas and the Silesian University of Technology for the support provided to the development of this study.

## Nomenclature

BDC bottom dead centre  
BMEP brake mean effective pressure

CH<sub>4</sub> methane  
COV coefficient of variation

H <sub>2</sub>	hydrogen	SI	spark ignition engine
IMEP	indicated mean effective pressure	T	temperature
l <sub>o</sub>	specific cycle work	TDC	top dead center
LHV	lower heating value	V	volume
p	pressure	λ	excess air ratio

## Bibliography

- [1] Ahmad A, Yadav K, Hasan S. Biogas as a sustainable and viable alternative fuel for diesel engines: a comprehensive review of production, purification, and performance evaluation. *P I Mech Eng D-J Aut.* 2024;238:325-345. <https://doi.org/10.1177/09544089241255930>
- [2] Aktaş F. Performance and emission prediction of hydrogen addition to natural gas powered engine using 0/1 dimensional thermodynamic simulation. *International Journal of Energy Studies.* 2022;7:67-81.
- [3] Conklin C, Szybist P. A highly efficient six-stroke internal combustion engine cycle with water injection for in-cylinder exhaust heat recovery. *Energy.* 2010;35:1658-1664. <https://doi.org/10.1016/j.energy.2009.12.012>
- [4] Fuwu Y, Lei X, Yu W. Application of hydrogen enriched natural gas in spark ignition IC engines: from fundamental fuel properties to engine performances and emissions. *Renew Sustain Energy Rev.* 2018;82:1457-1488. <https://doi.org/10.1016/j.rser.2017.05.227>
- [5] Ghazi K. Hydrogen as a spark ignition engine fuel. *Int J Hydrog Energy.* 2002;28:569-577. [https://doi.org/10.1016/S0360-3199\(02\)00150-7](https://doi.org/10.1016/S0360-3199(02)00150-7)
- [6] Iafrate N, Matrat M, Zaccardi M. Numerical investigations on hydrogen-enhanced combustion in ultra-lean gasoline spark-ignition engines. *Int J Engine Res.* 2021; 22:375-389. <https://doi.org/10.1177/1468087419870688>
- [7] Lee S, Yi H, Jang H, Park C, Kim C. Evaluation of emission characteristics of a stoichiometric natural gas engine fueled with compressed natural gas and biomethane. *Energy.* 2021; 216:19376. <https://doi.org/10.1016/j.energy.2021.119766>
- [8] McTaggart-Cowan P, Rogak N, Munshi R, Hill G, Bushe K. Combustion in a heavy-duty direct-injection engine using hydrogen–methane blend fuels. *Int J Engine Res.* 2009;10. <https://doi.org/10.1243/14680874JER02008>
- [9] Rasi S, Läntelä J, Rintala J. Trace compounds affecting biogas energy utilization – a review. *Energy Conv Manag.* 2011;52: 3369-3375. <https://doi.org/10.1016/j.enconman.2011.07.005>
- [10] Sierens R, Demuyneck J, Vancoillie J, Sileghem L, Verhelst S. Efficiency comparison of hydrogen fuelled IC engines with gasoline and methanol fuelled engines. Conference proceedings of Hypothesis IX (paper HYP-024), San José, Costa Rica. 2011.
- [11] Swinbourn N, Li C, Wang F. A comprehensive review on biomethane production from biogas separation and its techno-economic assessments. *Chem Sus Chem.* 2024;17:1-37. <https://doi.org/10.1002/cssc.202400779>
- [12] Teoh Y, How H, Le T, Nguyen H, Loo D, Rashid T et al. A review on production and implementation of hydrogen as a green fuel in internal combustion engines. *Fuel.* 2023;333: 126525. <http://doi.org/10.1016/j.fuel.2022.126525>
- [13] Turns R. An introduction to combustion: concepts and applications. 3rd ed. McGraw-Hill, New York 2012.
- [14] Verhelst S, Wallner, T. Hydrogen-fueled internal combustion engines. *Prog Energy Combust Sci.* 2009;35:490-527. <https://doi.org/10.1016/j.peccs.2009.08.001>
- [15] Wróblewski P, Bratkowski P. Effect of using a combination of coatings on reducing structural defects in the working area of the combustion chamber and on the energy efficiency of a reciprocating internal combustion engine. *Combustion Engines.* 2025;202(3):118-130. <https://doi.org/10.19206/CE-207651>

Prof. Willian Nadaleti, DSc., DEng. – Engineering Center, The Federal University of Pelotas, UFPel, Brazil.  
e-mail: [willian.nadaleti@ufpel.edu.br](mailto:willian.nadaleti@ufpel.edu.br)



Prof. Ireneusz Szczygiel, DSc., DEng. – Institute of Thermal Technology, Silesian University of Technology, Poland.  
e-mail: [ireneusz.szczygiel@polsl.pl](mailto:ireneusz.szczygiel@polsl.pl)



Prof. Grzegorz Przybyła, DSc, DEng. – Institute of Thermal Technology, Silesian University of Technology, Poland.  
e-mail: [grzegorz.przybyla@polsl.pl](mailto:grzegorz.przybyla@polsl.pl)

